

FAILURE CRITERIA FOR NON-METALLIC MATERIALS PART II: CERAMIC MATRIX COMPOSITES

C. Kaiser¹, H. Weihs², H. Wittke³ and A. Obst⁴

¹ HPS GmbH, Christian-Pommer-Str. 34, 38112 Braunschweig, Germany

² DLR, German Aerospace Center, Pfaffenwaldring 38-40, 70569 Stuttgart, Germany

³ Invent GmbH, Christian-Pommer-Str. 34, 38112 Braunschweig, Germany

⁴ ESA/ESTEC, Keplerlaan 1, 2200 AG Noordwijk ZH, The Netherlands

ABSTRACT

The paper presents results from an ESA funded study on failure criteria for non-metallic materials with focus on CMC. Aim of the study was to get an overview of the state-of-the-art and to identify needs for new test methods to analyze multi-axial states of stress. A new test set-up using solid test samples with an optimized shape for analyzing combined tension/shear load cases has been developed. The test results have shown, that the interaction between intra-laminar shear and tensile stress is not of such kind as expected and predicted in test programs using tubular specimen. Therefore, new failure criteria have to be developed in the future to compensate deficiencies of the usual used polynomial failure criteria like ZTL and Tsai-Wu. The test results allow proposing to use maximum stress criterion as a practical approach for design work of CMC structures for combined tension/shear load cases.

1. INTRODUCTION

The need to build lighter and stiffer structures and components for spacecraft and launcher applications has stimulated the development of composites that perform better than conventional materials. Specific properties, fatigue, operational temperature, and thermal stability are improved substantially. However the knowledge on failure criteria, in particular for non-polymer based composites, is still limited. A better understanding of these failure criteria is required to further the development of composites.

Within the frame of the study “Failure Criteria for Non-Metallic Materials” funded by ESA detailed guidelines for the proper use of failure criteria during the different phases of composites spacecraft structures design have been elaborated for non-metallic materials. The part of the results that focuses on CMC is presented in this paper.

One of the most significant differences of composite spacecraft structures to common composite structures is the operational temperature range. On the one hand there are cryogenic composite structures with still open questions regarding the material properties at low temperatures; on the other hand especially CMC is mainly used for temperature protection systems in re-entry vehicles having very high temperature gradients leading to complex thermo-mechanical loading conditions inside of the structure. For the engineers it is of interest what kind of failure will happen and at which load first ply failure or ultimate failure occurs leading to the margin of safety. Part I [1] is focussing on Fibre Reinforced Plastics (FRP) and Part II on Ceramic Matrix Composites (CMC). This Part II shall give an comprehensive overview on existing failure criteria for CMC, which are available in significant lower number, have lower maturity and a lower level of experimental verification comparing to FRP (see Part I), and present results from a preliminary evaluation of these failure criteria and from a test program especially designed for biaxial testing (tension/shear) at high temperatures using a new designed test specimen.

2. MATERIAL CHARACTERISTICS OVERVIEW

Many types of fibres and matrices are used as constituents for CMC, typically Carbon and silicon carbide fibres and matrices. Regarding high temperature oxidation stability, silicon


carbide (SiC) is a well suited matrix system. Composites with ceramic matrix have been mainly designed for the application as load-bearing structures in the case of high and very high temperatures (2000°C or more). The mechanical behaviour and the failure behaviour are strongly influenced by the architectures of the CMC, e.g. structures designed by stacking of unidirectional reinforced layers or woven or braided structures. Two-dimensional (2D) woven fabrics are of special interest due to their ease manufacturability. The manufacturing process - e.g. chemical vapour infiltration (CVI), liquid polymer infiltration (LPI) or liquid silicon infiltration (LSI) - and the respective process parameters during manufacturing have a substantial influence on the mechanical properties and the failure behaviour. Therefore and in contrast to FRP, material data are always linked to the manufacturing process and typically cannot be derived from the data of the single CMC constituents.

In general, the matrices of CMC are characterised by a brittle material behaviour. Due to the processing of CMC at high temperatures and the additional cooling to room temperature micro cracks and pores are caused in the matrix and therefore inherent to the material. A result of the initial crack density is the so-called “quasi-ductile” or “damage-tolerant” failure behaviour of this material class. In the literature typical material parameters of the different types of CMC are quite well documented, but mainly measured at room temperature, which is not the typical temperature application range.

For determination of material properties, various test methods have been established such as uni-axial monotone and cyclic tests. It is to mention that numerous standard test methods exist for CMC and their constituents. A list of standard tests is given e.g. in [2]. Due to the application of CMC at high temperatures, the influence of temperature is of special interest: Some CMC as e.g. C/C-SiC show no degradation in the mechanical behaviour up to very high temperatures. In general, the macroscopic stress-strain curves for CMC are characterised typically by a non-linearity. The fatigue behaviour of a ceramic composite can be characterised by several features, such as e.g. stress-strain hysteresis, modulus degradation, strain ratchetting, and S-N behaviour.

Continuum Damage Mechanics (CDM) is used to calculate stresses and strains in CMC due to the non-linear material behaviour. Different CDM models are proposed in the literature, see e.g. [3], [4], [5] and [6]. A summary concerning some investigations of the thermo-mechanical material behaviour of C/C-SiC which has been studied in the research program SFB 259 of the German Research Foundation (DFG) is given in [7].

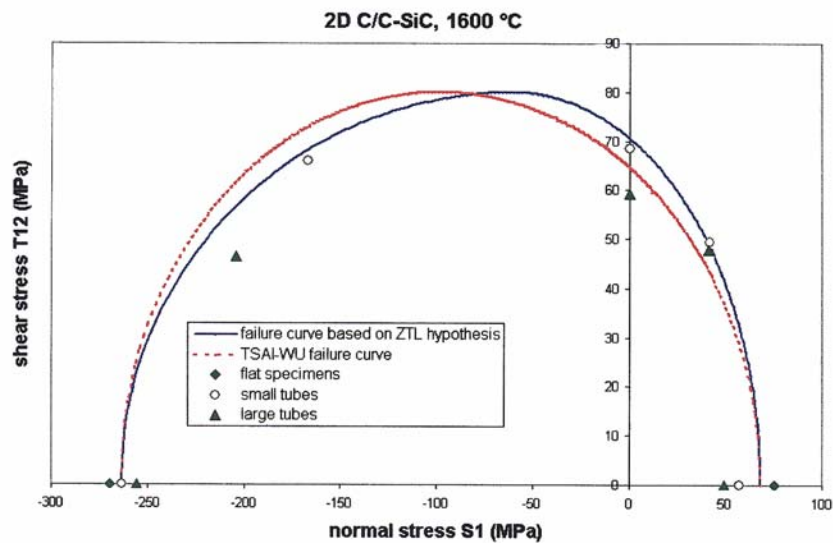
3. FAILURE CRITERIA STATE OF THE ART

 Comprehensive literature search on failure criteria used for the analysis of CMC was performed. A number of specially developed failure criteria for CMC exist. However, frequently also conventional failure criteria for fibre reinforced plastics are applied to CMC.

Typically maximum stress or strain criteria are first choices for evaluating the strength capability of composite material. Classical failure criteria which are based on continuum mechanics are not always appropriate for an application in the field of CMC.

For bi-axial stress and failure evaluation, the polynomial failure criterion of Tsai-Wu [8] is used as for FRP. But also other simple polynomial failure criteria can be used as shown by Geiwiz et al. [9], [10]: Here, the mathematical description of a (σ_1, τ_{12}) -

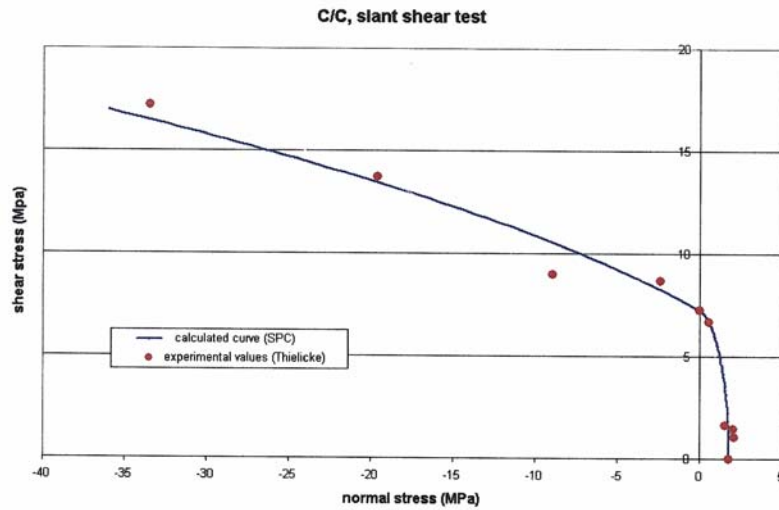
failure curve for C/C-SiC at 1600°C is based on the so-called ZTL hypothesis. In connection with a CDM analysis for the plane stress state, the Tsai-Wu failure criterion was used by Fink [7] for 2D C/C-SiC materials. A comparison of the ZTL failure curve derived in [9] and a Tsai-Wu failure curve for C/C-SiC at 1600°C is shown in Fig. 2. Comparing with experimental results, one can see clearly, that the ZTL criterion allows for slightly more realistic predictions than Tsai-Wu. Both criteria show a strong interaction for tension/compression and shear. However, CMC can show a better material behaviour at high temperatures. Therefore, using RT material data is a conservative way for designing CMC structures.



“Fig. 1. Comparison of two different failure curves for C/C-SiC at 1600°C with experimental data [9].”

First applications of the physical based failure criterion developed by Puck for FRP [11], [12] on Ceramic Matrix Composites can be found in [13]. The (σ_2, τ_{12}) -failure curve in case of unidirectional reinforced carbon fibre silicon carbide composites is experimentally determined demonstrating the possible applicability of the failure criteria of Puck also for this composite material class. Although Puck’s physically based failure criterion is very well established and experimentally verified for FRP, there are doubts of transferring the criterion to CMC due to the fact, that CMC shows other failure mechanics than FRP, which is the stringent basis of Puck’s failure theory.

The influence of the inter-laminar shear stress was investigated for the case of C/C composite CF 222 by Thielicke [14]. A special test method called Slant-Shear-Test has been developed for the determination of the ILSS. Its results lead to the part of a failure curve in the (σ_1, τ_{13}) -area as shown in Fig. 2. In addition, an inter-laminar failure criterion which is based on a fracture mechanical approach is proposed.

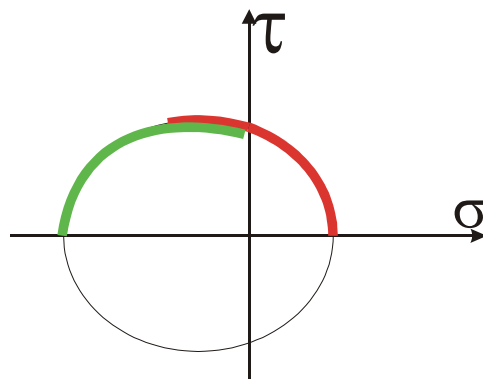


“Fig. 2. Comparison of calculated failure curve and experimental values from [14] for a C/C composite.”
 In contrast to FRP, there are only few data concerning failure curves or failure surfaces of CMC. Especially, a comparison of failure criteria for ceramic matrix composites as done for FRP [14] is almost not possible up to now. That means that tests for the derivation of data for failure criteria are essential.

4. EXPERIMENTAL WORK GOAL

A very important goal within the frame of the study was that test data should be derived relevant for practical use in the design of real structures. Many tests which are useful in the case of FRP are also useful in the case of CMC although modifications may be needed and standards for the case of CMC testing have to be taken into account. For uni-axial testing, flat specimens are usually used. Looking at bi-axial test methods, there are only few possibilities. Most of the bi-axial test results have been derived using filament wound tubes. However, the winding process for tubes differs significantly from the lamination process for plates and as already mentioned, the manufacturing technology has a significant influence on the material behavior and characteristics. Therefore, results taken from tubular specimen have to be evaluated critical w.r.t. applicability to laminated CMC material.

As already mentioned, in [14] significant effort has been invested in bi-axial testing of flat CMC samples by using the Slant-Shear-Test-Method to derive combined (σ_1, τ_{13})-strength values. This test method can be applied also to derive intra-laminar strength values under combined compression. Due to the sensitive behavior of CMC w.r.t. tension this test method is limited to compression/shear tests only. One of the main goal of the study was to derive a new test-method and test sample geometry to be able to apply combined tension and shear on representative samples in the sector of tension/shear (see Fig. 3).



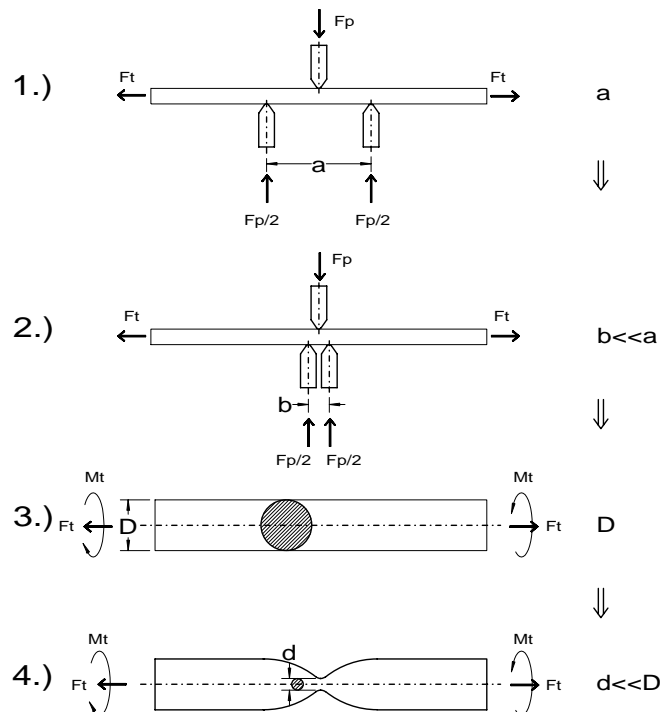
“Fig. 3. Comparison of bi-axial test ranges of Slant-Shear-Test-Method (green, limited to compression/shear only) and proposed new test method (red, covering mainly tension/shear).”

5. TEST SAMPLE EVOLUTION

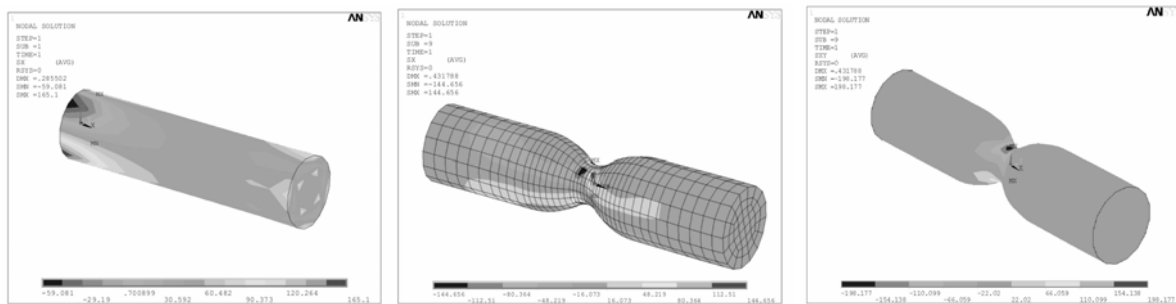
Since most high-temperature CMC structures are fabricated from plates or made as curved shells with high in-plane property values and lower values in transverse direction, it was decided to manufacture also the samples from plates. Such samples could have rectangular or circular cross section. The simplest type of sample is the flat sample with rectangular cross section. In this case, to have a bi-directional load condition, a transverse load is applied simultaneously with a normal load in order to obtain the intended state of stress (Fig. 4 case 1. and 2).

Using the finite element method with material property values taken from previous tests [15] that type of test was analyzed first. The results showed that the bending stress dominates and leads to a premature failure. By reducing the distance between the load introduction points significantly, failure critical stress levels for tension from bending and shear can be reached. However, the load introduction points are then so close together that the area with high shear stress becomes very small. This results in high stress gradients so that it is difficult to identify an area with a clear multi-axial stress state from which allowables can be derived. In addition, the introduction of high loads over a very small distance on thick samples at high temperature is in practice a difficult task.

Another solution studied was to use full cylindrical samples (Fig. 4 case 3) which are subjected to combined torsion moment and axial load. In this case high stress peaks are generated at the load introduction area due to the tension and compression loads (see Fig. 5).



“Fig. 4. Evolution of test principles and test samples geometry.”



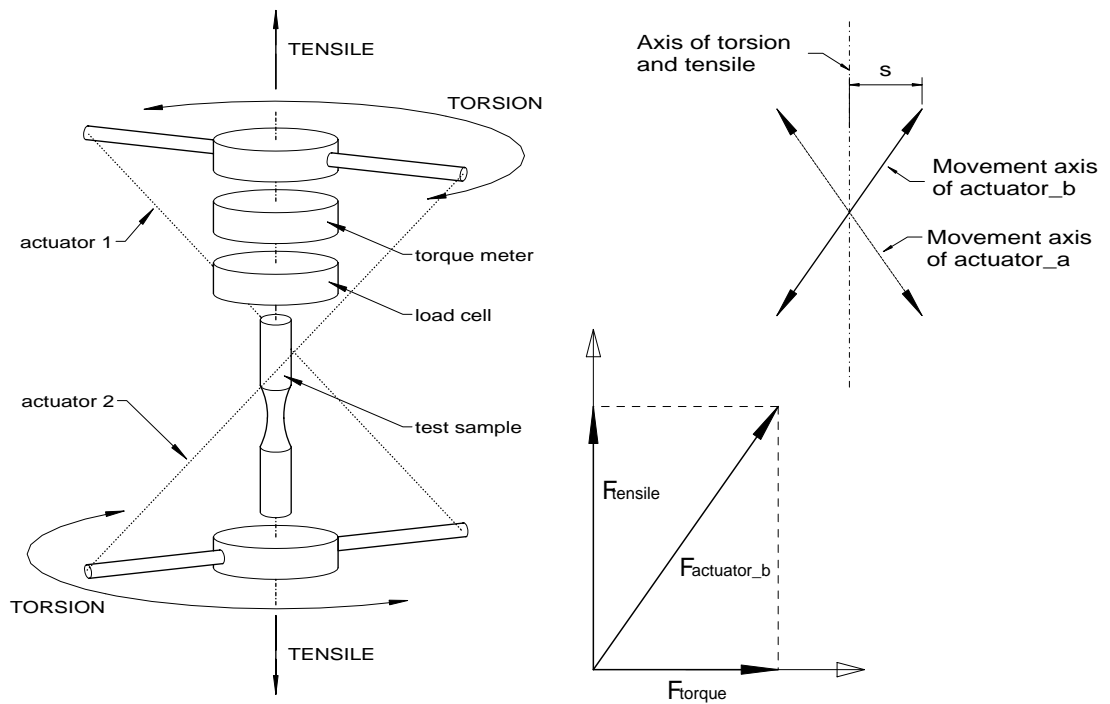
“Fig. 5. Numerical results from FE-analysis for tension and compression on a cylindrical rod (left) and tension and compression (middle) and shear (right) on an hourglass shaped sample.”

Even if the stress peaks could be reduced by specific design solutions, the load introduction area would be subjected to higher loads than the mid section of the sample. Considering that the samples are heated in the mid section for high temperature test, this type of geometry is therefore not suitable for the intended investigations since the sample would fail definitively at the load introduction.

Further investigations resulted into another approach with a sample of a tailored cross section area in its mid section (hourglass shape, Fig. 4 case 4). By optimization of the geometry of the cross-section it can be ensured that the fracture location will be in the test section that is in the high-temperature region. Further, a favourable distribution of tension/compression stresses in comparison to the shear stresses caused by a torsion moment can be observed (see Fig. 5). The shear stresses can be brought up to a failure critical level which is necessary for the investigations of multi-axial load conditions as envisaged whereas the tension and compression stresses remain on the level observed also with the cylindrical samples that were analyzed.

6. TEST SET-UP

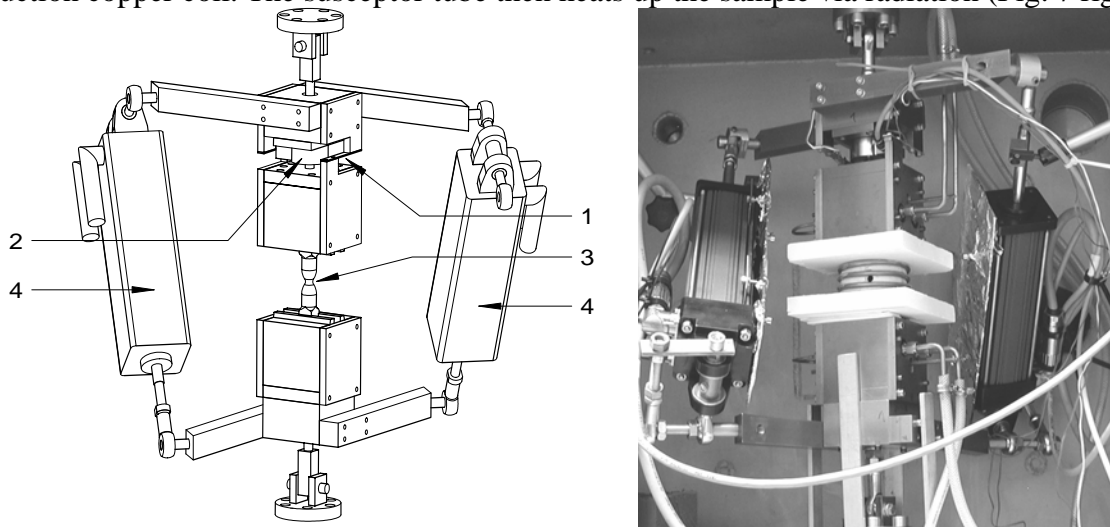
The basic idea for the test set-up is to have a universal tool to determine material property values. With regard to the numerical work this is achieved by using a suitable sample geometry that can be easily analyzed to correlate with test results. Therefore, a test fixture was designed that can be used in different test equipment. For this reason the torsion moment acting on the sample has to be reacted by the device itself and not by the machine. Furthermore, no constraining forces must be generated by guides or bearings. The device works as follows: Two linear actuators generate a rotation due to their off-axis position in the device as illustrated in Fig. 6.



“Fig. 6. Set-up for combined tension-torsion loading test device.”

In addition to the rotation generated by the torsion moment, an axial force component is also applied by the testing machine itself. The load cell (Fig. 7 no. 2) is positioned between the torsion moment load introduction and the sample. This requires a force-controlled operation of the machine. The whole device is integrated into the machine using cardan joints so that no additional moments or side effects can act on the sample. The actuators are controlled with dedicated software that constantly measures the real torsion moment acting upon the sample and adjusts it to the requested value.

The measurement of the torsion moment is carried out using the elongation of two aluminium strips equipped with strain gauges (Fig. 7 no. 1). The sample (Fig. 7 no. 3) is clamped with water cooled jaws at the quadratic sample ends. In the mid section the sample has a circular cross section and is indirectly heated via induction heating. Indirectly means that a graphite susceptor tube is heated via eddy current induced by the electromagnetic field generated by an induction copper coil. The susceptor tube then heats up the sample via radiation (Fig. 7 right).

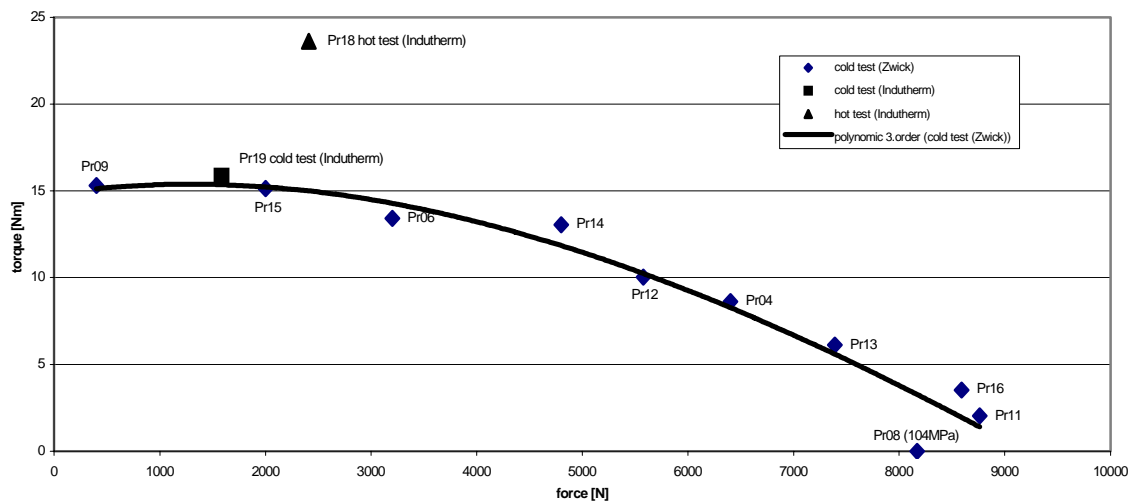


“Fig. 7. Sketch (left, without cooling and heating coil) and picture (right, including susceptor tube and induction coil) of test device.”

7. TEST RESULTS

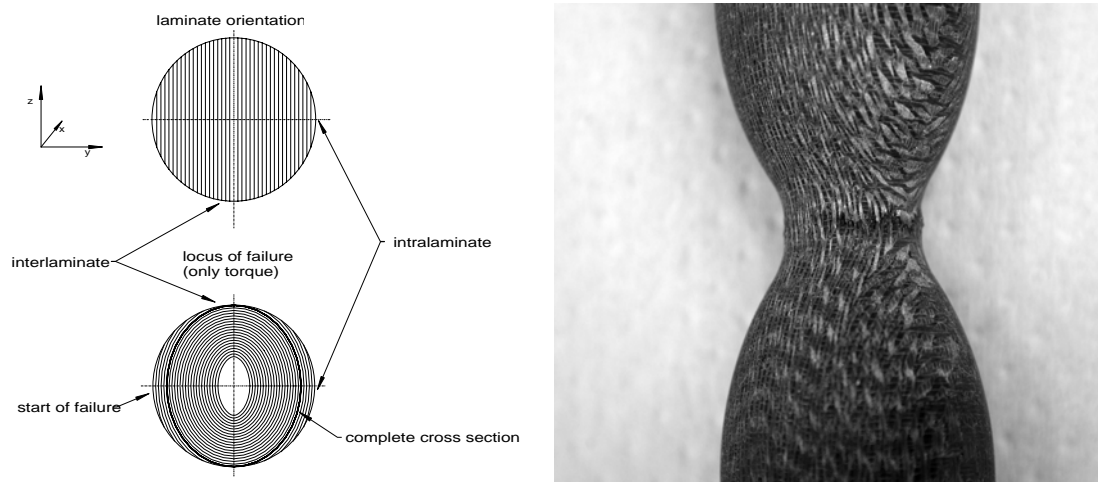
Two different test strategies are possible. One is that a tensile load is applied and kept at a constant level and then the torsion moment is increased until fracture of the sample. The other approach is to keep the torsion moment constant and to increase the tensile load until fracture. Depending on the load combination, one of the two strategies is applied to keep variations in the results small. During tests with a high torsion moment, the tensile load was kept constant, during tests with a high tensile load the torsion moment was kept constant.

Fig. 8 shows the results of all room temperature tests. All samples were manufactured from one batch of C/C-SiC material that is produced via the liquid silicon infiltration process at DLR [16]. A first test series (sample Pr04-Pr17) was performed at room temperature in a ZWICK machine. Another one with high torsion moment show a clear failure process (samples Pr09, Pr15, and Pr19). The crack is initiated in the intra-laminar mode due to the higher shear stiffness at this location (due to plate lay-up) and then continues to grow around the circumference until inter-laminar failure occurs. This type of failure is shown in Fig. 9.

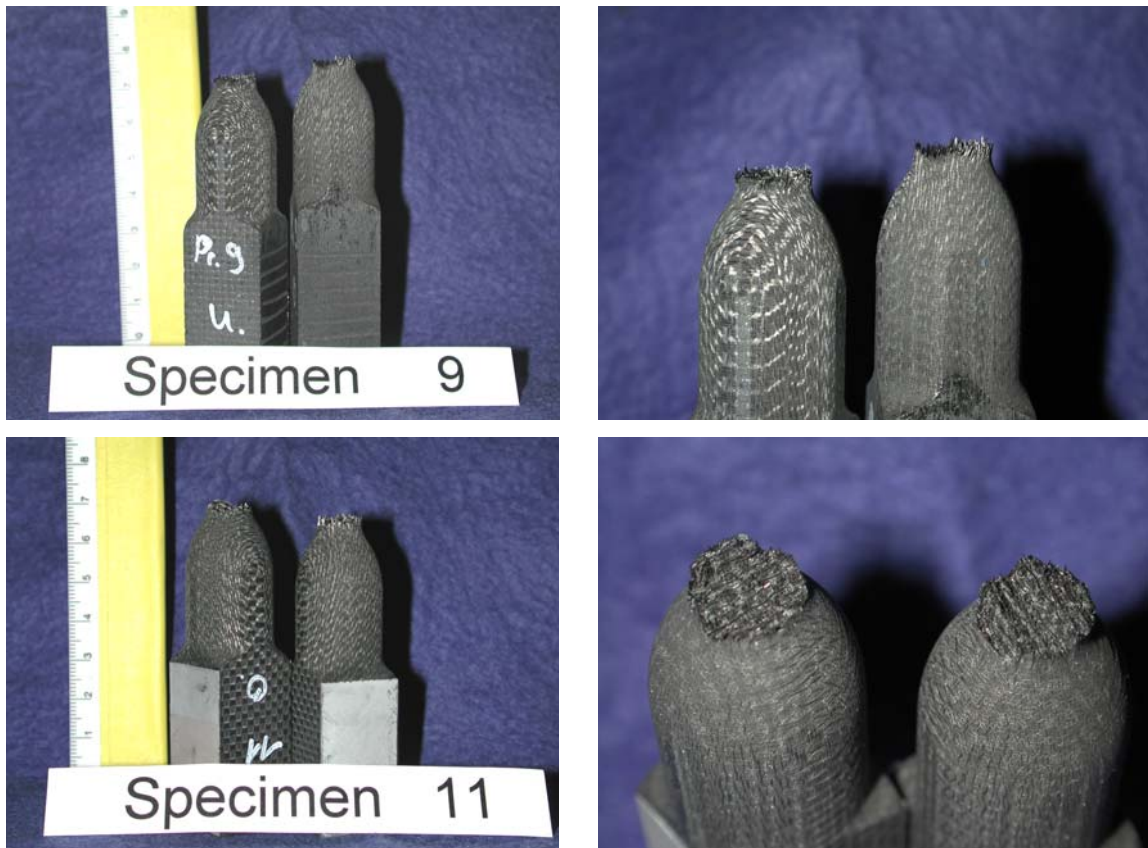


“Fig. 8. Test results.”

The pictures in Fig. 10 show the cracked samples identifying clearly the different shape of fracture plane. Specimen 9 failed due to high tensile loads and specimen 11 due to high shear loads.



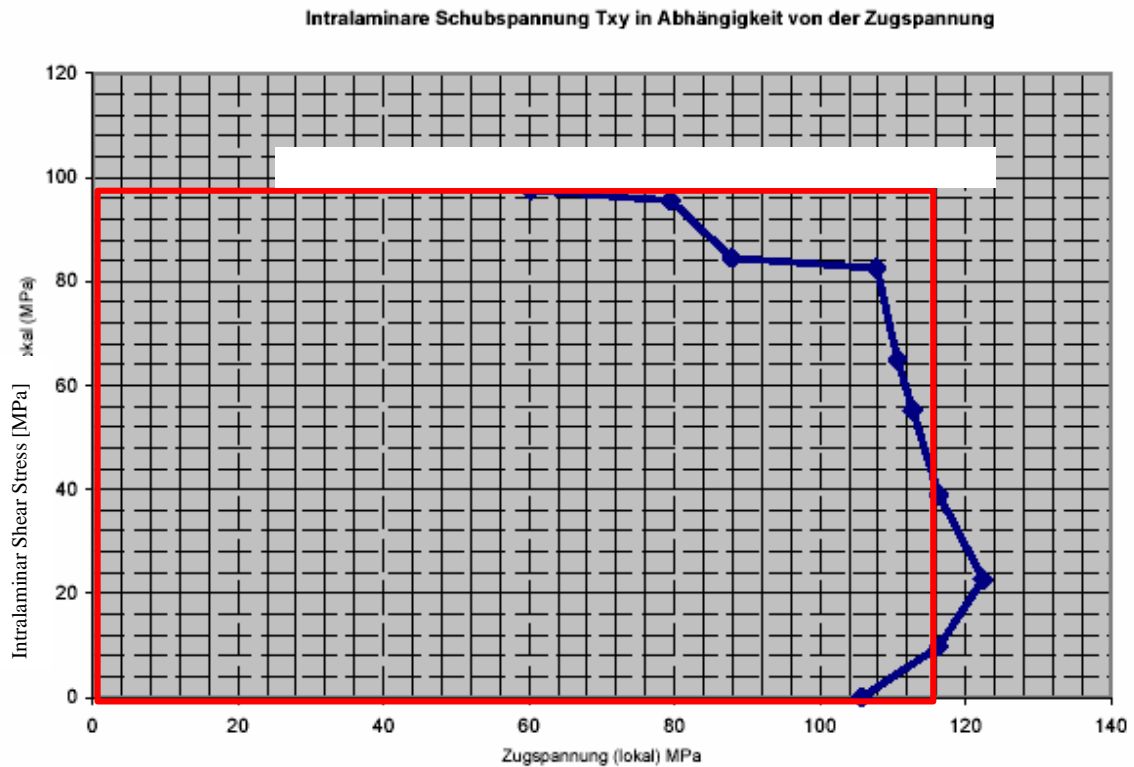
“Fig. 9. Crack propagation due to too high intra-laminar stresses (left) and crack observation on sample.”



“Fig. 10. Tested RT specimen.”

Re-calculating the respective tension and shear stresses from the test results of Fig. 8, one can now generate a failure curve for the tension/shear interaction as shown in Fig. 11 by the blue line which differs significantly from the one shown in Fig. 1. The interaction is different than that predicted by e.g. the ZTL-criterion or the Tsai-Wu criterion. The observed failure behavior looks more in a way that tension failure is not significantly influenced by an increased shear load and vice versa. That means that the test data show more commonalities with the maximum stress failure curve as indicated in Fig. 11 by the rectangular red box. Only in case of high shear and high tension loads a clear interaction can be observed but more in a way of a typical rounding effect.

That means, that at least for tension/shear (σ_1 - τ_{12}) interaction the observed higher combined strength values will not be predicted by the ZTL or Tsai-Wu failure criterion. Therefore, a design based on strength analysis using these polynomial failure criteria would be too conservative and lead to not use the full material capability and a non-optimum design.



“Fig. 11. Failure curve (blue) derived from experimental data comparing to maximum stress failure curve (red).”

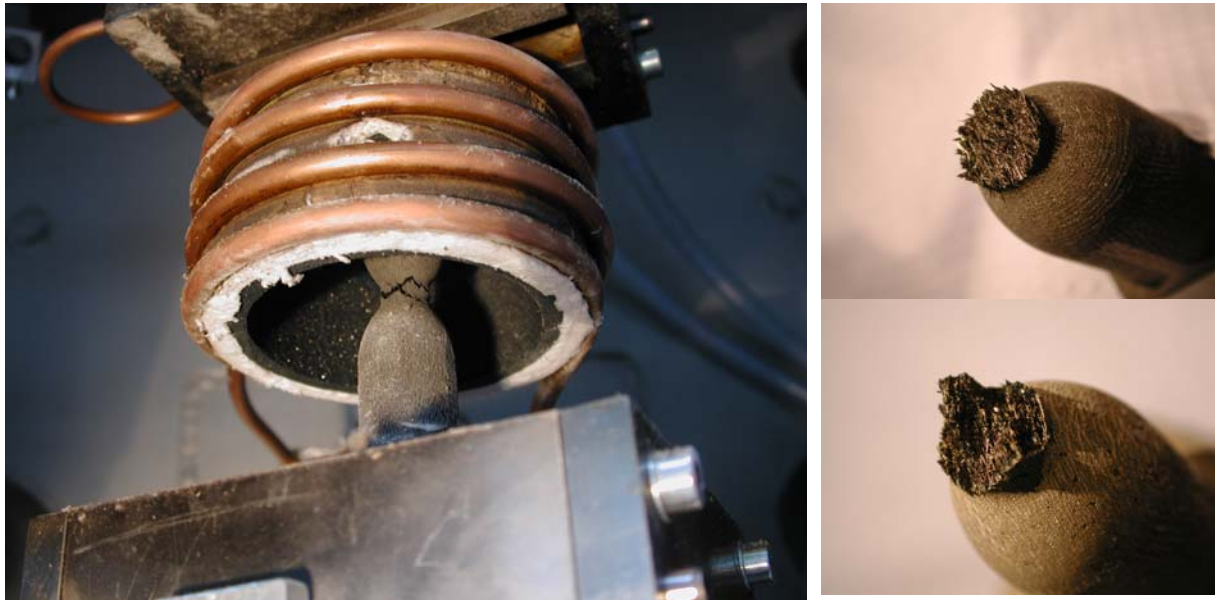
8. HIGH TEMPERATURE TESTS Tensile Stress [MPa]

The presented test set-up is designed to be used also in the high temperature Indutherm test machine [17], which was verified by the results from sample Pr19 (see Fig. 8) that fit perfectly to the results acquired from samples Pr01 - Pr17 in the ZWICK machine. There is enough space around the sample to install a heating device and insulation to heat up samples up to very high temperatures. One test was carried out at 1400°C and the machine has been used in previous programmes at temperatures of more than 1600°C. For Pr18 (see Fig. 8) sample failure with high torsion moments applied was observed at significant higher shear strengths than for an identical RT test on sample Pr19. The higher shear strength at high temperature is in line with earlier results [15] that state increased shear strength of up to 60% higher than at RT.

The work in the near future will concentrate on a more exact determination of the shear modulus and related Poisson’s ratio both for intra- and inter-laminar shear to obtain a better correlation between tests and analysis. With the respective shear strength values the failure surface can then be described for the tension/shear region.



“Fig. 11. High temperature test campaign.”



“Fig. 12. Test sample after high temperature test.”

9. CONCLUSIONS

The new developed testing device and hourglass test specimen cut out from flat CMC material allows for application of tension and shear in all possible combinations and to derive a full set of test data in the complete $(+\sigma_1/+\tau_{12})$ -range. The observed failure behaviour is different of the ones observed with tubular specimen and results in higher combined strength values for both RT and HT. The new test method will allow determining a wide range of material data especially for combined load cases.

The (σ_1, τ_{12}) -failure curve generated from a first collection of test data cannot confirm the strong tension/shear interaction as predicted by typical polynomial failure criteria like ZTL and Tsai-Wu. The interaction is only significantly apparent at high stress levels for both tension and shear. At intermediate and lower levels of tension or shear failure is dominated more by maximum shear or tension stress respectively. Therefore, margins for optimization of CMC structures have been identified and the material characteristics are better than expected

and predicted in previous publications and test campaigns. A clear need to develop new failure criteria is identified which predict correctly the observed failure behaviour.

Finally, a practical approach for design work and estimation of failure loads is to use a maximum stress criterion. This approach is similar to the design using monolithic ceramics. Having a ceramic based material, this should not be a surprise. However, the Weibull modulus is completely different. It is very important for the design engineer to have more reliable strength values and not a statistic probability like monolithic ceramics.

ACKNOWLEDGEMENT

The presented work was funded by the European Space Agency (ESA) under contract no. 16162/02/NL/CP.

References

1. **Kaiser, C., Kuhnel, E. and Obst, A.**, "Failure Criteria for Non-Metallic Materials – Part I: Fiber Reinforced Plastics", *Proceedings of the ECCM11*
2. **N. N.**, "Composite Materials Handbook, Volume 5: Ceramic Matrix Composites (MIL-HDBK-17-5)", DAPS, Philadelphia, USA, 2002.
3. **Hald, H.**, "Fiber reinforced ceramics for hot structures of reentry vehicles – simulation, test and comparison with experimental flight data", *Ph.D. thesis*, University of Stuttgart, (Forschungsbericht 2001-17, Deutsches Zentrum für Luft- und Raumfahrt e.V.), 2001, in German.
4. **Shan, H., Pluvinage, A., Parvizi-Majidi, A. and Chou, T.**, "Damage Mechanisms of two-dimensional woven SiC/SiC composites", *Journal of Engineering Materials and Technology*, **116** (1994), 403–407.
5. **Weigel, N.; Kröplin, B. and Dinkler, D.**, "Micromechanical Modelling of damage and failure mechanisms in C/C-SiC", *Computational Materials Science*, **16** (1999); 120-132.
6. **Chaboche, J.-L. and Maire, J.-F.**, "A new micromechanics based CDM model and its application to CMC's", *Aerospace Science and Technology*, **6** (2002), 131-145.
7. **Fink, A.**, „Ein Grenzflächenmodell zur Beschreibung des mechanischen Verhaltens faserverstärkter Keramiken“, *Ph.D. Thesis*, Institut für Statik und Dynamik der Luft- und Raumfahrtkonstruktionen (ISD); University of Stuttgart, 1995, in German.
8. **Tsai, S. and Wu, E.**, "A General Theory of Strength for Anisotropic Materials", *Composite Materials*, **5** (1971), 58-80.
9. **Geiwiz, W., Theuer, A. and Arendts, F.J.**, "Empirical Determination of a Failure Criterion for C/C-SiC", *Proceedings of the Third International Conference on Composites Engineering (ICCE/3)*, New Orleans, July 21-26, 1996, 297-298.
10. **Geiwiz, W., Theuer, A. and Arendts, F. J.**, „Experimentelle Bestimmung eines Versagenskriteriums für faserverstärkte Keramik“, *Proceedings of the DGM-Tagung Verbundwerkstoffe und Werkstoffverbunde*, Kaiserslautern, 17.-19. Sept. 1997, Kaiserslautern, in German.
11. **Puck, A.**, "Festigkeitsanalyse von Faser-Matrix-Laminaten, Modelle für die Praxis (Strength analysis of fibre-matrix/laminates, models for design practice)", Carl Hanser Verlag, Munich, 1996, in German.
12. **Puck, A. and Schürmann, H.**, "Failure analysis of FRP laminates by means of physically based phenomenological models", *Composites Science and Technology*, **58** (1998), 1045-1067.
13. **Hufenbach; W., Kroll, L., Langkamp, A. and Höpken, J.**, "Physically Based Failure Criteria for Long-Fibre Reinforced Ceramics", *Proceedings of High Temperature Ceramic Matrix Composites*, **4**, Munich, 1. - 3. October 2001, 564-569.
14. **Thielicke, B.**, "Determination of the Interlaminar Shear Strength of Carbon Fibre reinforced Carbon using the Compression-Shear Test within the Temperature range of Room Temperature and 2000 C", *Ph.D. Thesis*, University of Karlsruhe, 1997, in German.
15. **Geiwiz, W.**, "Thermomechanisches Verhalten von C/C-SiC, Materialkennwertermittlung", Report SFB 259, TP B1; University of Stuttgart, 1995, 123-148, in German.
16. **Krenkel, W. and Fabig, J.**, "Materialentwicklung und Herstelltechnologie für C/C-SiC Bauteile", Report SFB 259, TP B2a; University of Stuttgart, 1998, 147-168, in German.

17. **Ortel, M., Weihs, H. and Fischer, I.**, "Thermo-Mechanical Qualification Tests of complex CMC Re-Entry Structure"; Proceedings of the 27th International Cocoa Beach Conference and Exposition, 25-31 January, 2003 Cocoa Beach USA